

$\alpha(P = e+p)$ . Data  $\alpha(T, e, p)$  were taken covering the following range of parameters:

temperature	$T = 316 \text{ to } 282 \text{ K};$
vapor pressure	$e = 0 \text{ to } e_1 \text{ (RH} < 95\%); \text{ and}$
total pressure	$P = e_1 + p$ , where $p = 0 \text{ to } 1200 \text{ torr (capacitance manometer)}$ , $p = 0 \text{ to } 3 \text{ atm (aneroid manometer)}^*$ .

Maximum vapor pressure  $e_1$  was determined by the temperature  $T_W$  of the water reservoir.

With the spectrometer performance optimized at  $P = 0$  (see Figure 3b), an additional set of problems appeared when the gas pressure was varied. Introducing and removing gas from an enclosure changes the temperature  $T_g$  of a sample (Figure 4). Only pressure scan rates below  $\pm 100 \text{ torr/min}$  ensured quasi-static gas conditions,  $T_g = T_C$ . Typically, the pressure was varied in steps. While the gas settled, the klystron frequency  $f_K$  was retuned to balance the baseline of  $A(t)$ .

Working with water vapor often brought disappointing results with respect to reproducibility. Condensation effects on both mirrors and pinhole coupling were avoided (see p. 5). One source was the "piston" effect where local compression condenses part of the vapor; another error source was the slow diffusion-mixing of water vapor with stagnant air. We calculated the diffusion time constant for vapor molecules to travel 30 cm inside the cell against 1 atm of dry air to be

$T$	(K)	315	300	285
$\tau_D$	(min)	5.4	6.0	6.7

It takes a period longer than  $5 \cdot \tau_D$  for a homogeneous moist air mixture  $P = e_1 + p$  to develop. A measurement of  $a(P)$  shown in Figure 5a indicates even longer time periods. Water pressure  $e_1(T_W)$  settled with no delay when the  $H_2O$ -valve was opened. Dry air injection first reduced  $e_1$  (piston effect) and then it took up to 1 hour to obtain a stable value  $a(e_1+p)$ . Mixing was accelerated to less than 5 minutes by installing a fan, driven by a magnetically coupled rotary vacuum feed-through.

---

\*Experimental pressure scale is measured in torr; the prediction model MPM uses the pressure unit  $1 \text{ kPa} = 10 \text{ mb} = 7.5006 \text{ torr}$ .

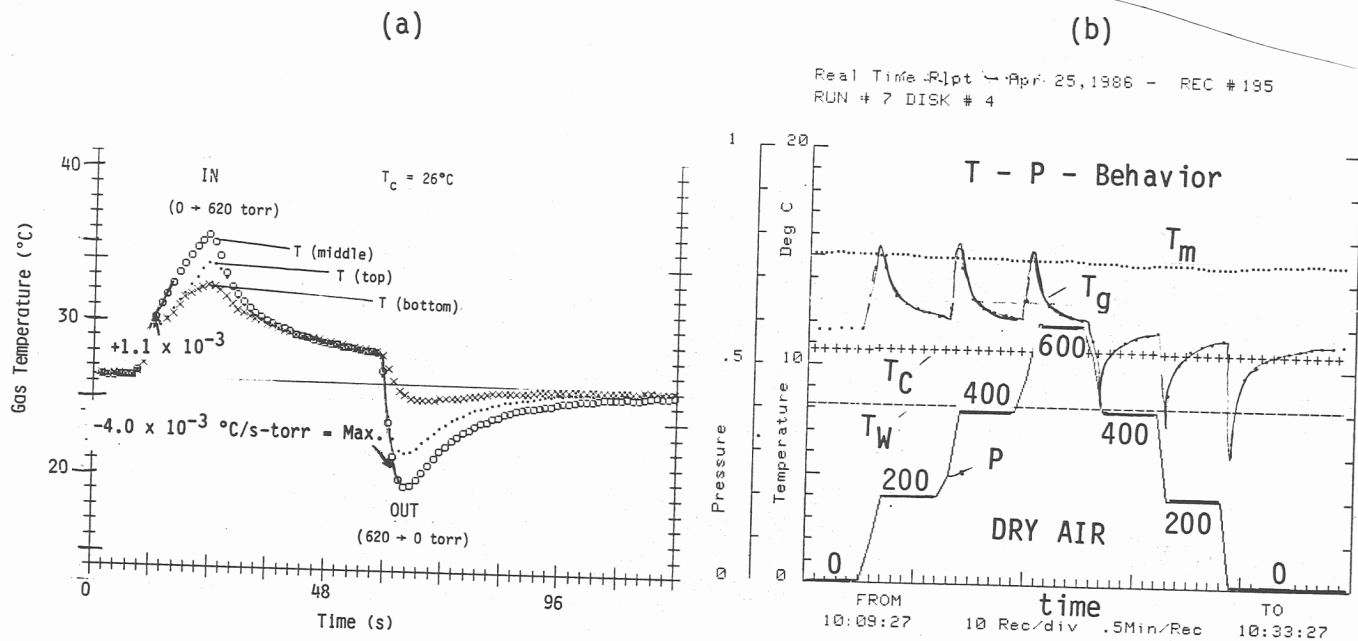


Figure 4. Temperature responses inside the spectrometer cell:  
(a) time-response test of gas temperature ( $T_g$ ) sensors,  
(b) temperature-vs.-pressure behavior for a typical dry air case.

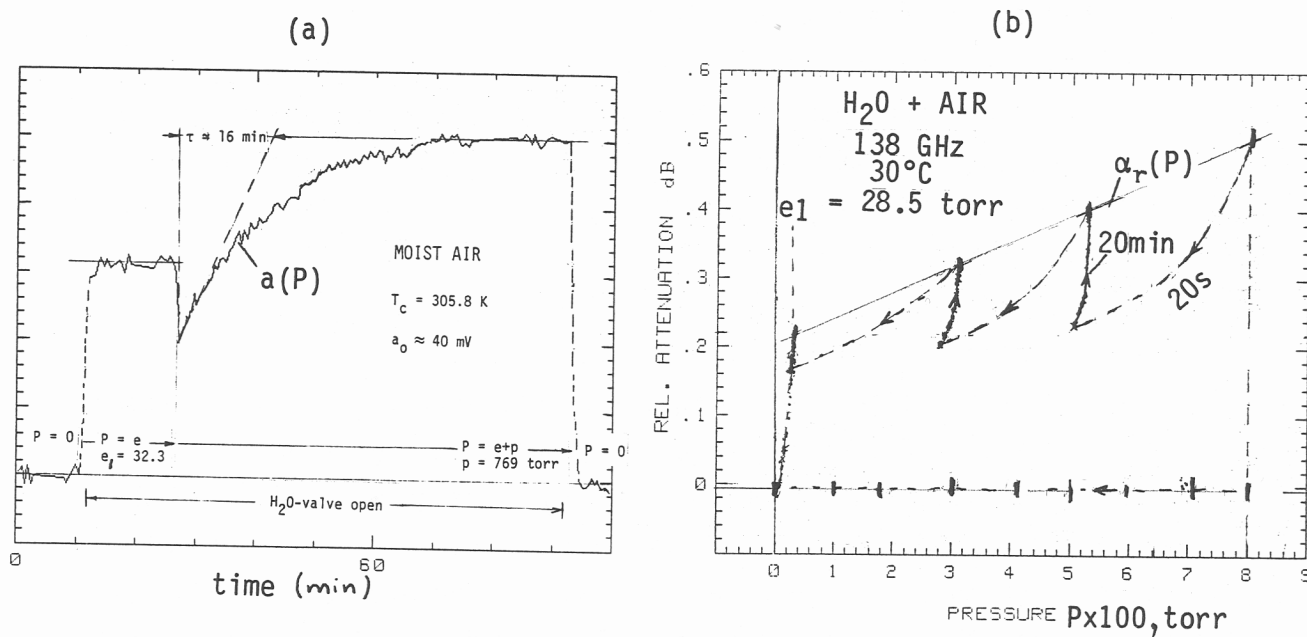


Figure 5. Mixing effects of H<sub>2</sub>O + AIR from time series of 138 GHz attenuation:  
(a) piston effect and diffusion mixing;  
(b) decompression condensation during pump-down over open vapor source.

One other effect was observed when dealing with moist air inside a vessel: reducing the total pressure  $P$  caused the water vapor to condense by decompression cooling. Even with the water vapor supply fully exposed to the air mixture, it took a long time (20 min) to reestablish the initial vapor pressure  $e_1$  as indicated by  $\alpha_r(P)$  in Figure 5b (mixing fan was off).

### 2.3 Water Vapor and Moist Air Attenuation Results

Moist air attenuation  $\alpha$  at a frequency  $f$  that falls within the millimeter-wave window range centered at 140 GHz, can be expressed by [6], [7]

$$\alpha = k_s(T) e^2 + k_f(T) ep + k_d(T) p^2 \quad \text{dB/km}, \quad (5)$$

where  $e$  and  $p$  in kPa are partial pressures of water vapor and dry air, respectively. Pressure-broadening theory of the  $H_2O$  rotational spectrum predicts ( $e > 0.01$  kPa) a fixed ratio  $m$  between air- $(ep)$  and self- $(e^2)$  broadening; i.e.,

$$m = k_f/k_s. \quad (6)$$

An extensive series of controlled laboratory measurements was performed at 137.8 GHz to determine the  $k$ -coefficients of (5) and (6). Table 1 is a summary of over 2500 individual data points  $\alpha(T, e, p)$ .

At  $T = 303$  K, the foreign-gas broadener AIR ( $p$ ) was replaced by its principal constituents  $N_2$ ,  $O_2$ , and Ar. These results are listed in Table 2. The broadening efficiency  $m$  is useful to explain  $H_2O$  absorption processes that support (5) since  $\alpha = k_s e (e+mp)$ . Pure oxygen ( $O_2$ ) measurements for pressures up to 2.4 atm against Ar as the "loss-free" reference provided an estimate of  $k_d$  when multiplying the result by 0.21.

Data of Table 1 were further reduced to a reference temperature  $T_0 = 300$  K. Temperature dependence of the  $k_{s,f,d}$  coefficients was fitted to a power law,

$$k(T) = k\theta^x \quad \text{dB/km-kPa}^2, \quad (7)$$

where  $\theta = 300/T$  is an inverse  $T$ -parameter.

The results for moist air attenuation at 137.8 GHz, when expressed by (5) to (7), led to

Table 1. Comparison between Measured (X) and Model-Predicted (M-MPM, see Section 3) Coefficients  $k_{s,f}$  of (5). Experimental conditions:  $f = 137.8$  GHz,  $T = 282-316$  K,  $P = e_i + p$ ,  $p = 0-110$  kPa

	T	$e_i$ (RH)	Moist Air			Dry Air
			$k_s$	$k_f$	$m$	$k_d$
	K	kPa	dB/km-kPa <sup>2</sup> x10 <sup>-2</sup>		x10 <sup>-2</sup>	dB/km-kPa <sup>2</sup> x10 <sup>-6</sup>
X	315.5	7.49 (90%RH)	8.01	0.485	6.06	-
M			7.85	0.481	6.13	1.93
X	305.9	4.45 (90%RH)	10.9	0.540	4.95	-
M			10.81	0.530	4.90	2.10
X	303.2	3.80 (90%RH)	12.0	0.558	4.65	2.2
M			11.84	0.545	4.60	2.11
X	296.1	2.51 (90%RH)	15.0	0.59	3.9	-
M			15.08	0.589	3.91	2.29
X	286.7	1.39 (90%RH)	21.0	0.65	3.1	-
M			21.22	0.649	3.06	2.46
X	281.8	1.05 (94%RH)	25.7	0.68	2.65	-
M			25.49	0.687	2.70	2.64

Table 2. Attenuation Measurements of Water-Vapor/Air-Constituent Mixtures (f=137.8 GHz, T=303 K, E<sub>1</sub>=3.80 kPa) Expressed with k<sub>x</sub>-Coefficients of (5), and Corresponding Broadening Efficiencies m<sub>x</sub> (6). Included are Line-core Measurements m<sub>L</sub> and their Predictions m<sub>1</sub> and k<sub>1</sub> Transposed to 138 GHz

	FAR WING (303K)				LINE CORE (300K)		
	$k_x$	$k_1$	$m_x$	$m_1$	$m_L$		
$f(\text{GHz})$	137.8		137.8		22.2	183.3	
<u>Species</u>	$\text{dB/km-kPa}^2 \times 10^{-2}$				[16]	[16]	[11]
	$\times 10^{-2}$				$\times 10^{-2}$		
H <sub>2</sub> O	12.0	2.55	100	100	100	100	100
AIR	0.558		4.65	<u>21.9*</u>	20.8	22.7	22.1( $\theta^{-0.6}$ )
N <sub>2</sub>	0.627		5.23	24.6	22.8	24.9	
O <sub>2</sub>	0.322		2.68	12.6	14.0	14.3	
Ar	0.222		1.85	8.7	11.4	10.3	
	Linewidth (MHz/kPa)				135.0	143.0	151.9( $\theta^{1.1}$ )

\*Reference value (line-core average)

$$\begin{aligned}
k_s(T) &= 0.133(4)\theta^{10.3(3)}, \\
k_f(T) &= 5.68(5)10^{-3}\theta^{3.0(4)}, \\
k_d(T) &\approx 2.2(5)10^{-6}\theta^{2.8},
\end{aligned}
\tag{8}$$

and

$$m = 0.0427/\theta^{7.3}.$$

Digits in parentheses give the standard deviation from the mean in terms of the final listed digits. Typical examples of data plots  $\alpha_r(e)$  and  $\alpha_r(e_1 + p)$  are exhibited in Figure 6. All experimental results supported the formulation in (5). Model predictions of the experimental data are given in Figure 14 (Section 3.4).

### 3. ATMOSPHERIC PROPAGATION MODEL MPM

(see Appendix A and B for Details)

Dry air and atmospheric water vapor are major millimeter-wave absorbers; so are suspended droplets (haze, fog, cloud) and precipitating water drops that emanate from the vapor phase. A practical model (designated program code: MPM) was formulated that simulates the refractive index  $\underline{n} = n' - jn''$  of the atmospheric propagation medium for frequencies up to 1000 GHz [1] - [3]. Since the interaction with a neutral atmosphere is relatively weak, the refractive index is converted into a refractivity in units of parts per million,

$$\underline{N} = (\underline{n} - 1) 10^6 \text{ ppm.}$$

#### 3.1 Features of the Program

A user-friendly parametric program was developed that calculates the values of the complex refractivity  $\underline{N}$  for atmospheric conditions as a function of the variables  $f$ ,  $P$ ,  $T$ ,  $RH$ ,  $w_A$  (A/B/C/D),  $w$ , and  $R$ , as listed in Appendix A (Section A.1.1).

The output of MPM are three radio path-specific quantities:

• attenuation	$\alpha(f)$	dB/km
• refractive delay	$\beta_0$	ns/km
• dispersive delay	$\beta(f)$	ps/km